

## Formation of polymersomes with double bilayers templated by quadruple emulsions†

Cite this: DOI: 10.1039/c3lc41112e

Shin-Hyun Kim,<sup>\*ab</sup> Jin Nam,<sup>c</sup> Jin Woong Kim,<sup>d</sup> Do-Hoon Kim,<sup>c</sup> Sang-Hoon Han<sup>c</sup> and David A. Weitz<sup>\*a</sup>

Polymersomes, vesicles composed of bilayer membranes of amphiphilic block-copolymers, are promising delivery vehicles for long-term storage and controlled release of bioactives; enhanced stability of the membrane makes polymersomes potentially useful in a wide range of biological delivery applications by comparison with liposomes. However, unilamellar structure is intrinsically fragile when subjected to external stress. Here, we report a microfluidic approach to produce polymersomes with double bilayers, providing higher stability and lower permeability than unilamellar polymersomes. To achieve this, we developed a new design of a capillary microfluidic device to produce quadruple-emulsion drops which serve as a template for the polymersomes-in-polymersomes. When two bilayers are attracted by depletion in polymersomes-in-polymersomes, the inner polymersomes protrude and bud, forming double bilayers. We confirm these structures are indeed double bilayers using microaspiration and selective doping of the leaflets with nanoparticles. The resultant polymersomes have great potential as highly stable and biocompatible microcarriers for robust encapsulation and storage of bioactives such as drugs, cosmetics and nutrients.

Received 3rd October 2012,  
Accepted 12th January 2013

DOI: 10.1039/c3lc41112e

[www.rsc.org/loc](http://www.rsc.org/loc)

### Introduction

The core-shell geometry of double-emulsion drops makes them potentially useful for making microcapsules for the purpose of encapsulation of active materials such as foods, drugs, cosmetics, and display pigments. Although such a core-shell structure is difficult to achieve using bulk emulsification, microfluidic technologies have enabled precise control of the size and number of cores and shells of double-emulsion drops.<sup>1,2</sup> Moreover, multiple-emulsion drops with even higher order can be produced in microfluidic devices through multi-step sequential emulsification or single-step emulsification, albeit only for a limited set of fluids.<sup>3-5</sup> A variety of monodisperse microcapsules has been produced by templates of such double- and multiple-emulsion drops. For example, polymeric or inorganic microcapsules with homogeneous or

heterogeneous membranes can be prepared by solidification of selected phases; this solidification is achieved by polymerization or evaporation.<sup>6-12</sup> One very promising microcapsule structure is the polymersome, which is a vesicle whose membrane is comprised of a bilayer of amphiphilic block-copolymers; polymersomes provide higher stability and lower permeability than liposomes due to the larger molecular weight of the polymeric amphiphiles, making them useful for a wide range of drug-delivery systems and for fundamental studies of cell functions.<sup>13,14</sup> Double-emulsion drops can serve as a template to produce such polymersomes with very uniform size.<sup>15,16</sup> In addition, the unprecedented control of microfluidic emulsification enables production of polymersomes with multiple compartments; these are potentially useful for storage and delivery of multiple distinct components while avoiding their cross-contamination.<sup>17-19</sup> Although the stability of polymersomes is enhanced by comparison to that of liposomes, they are nevertheless intrinsically fragile when subjected to mechanical or osmotic stress due to their membrane structure: amphiphiles are aligned in the form of a bilayer without any interpenetration. Their stability can be considerably enhanced by forming the membrane from multiple bilayers. However, this has never been accomplished in convenient fashion using microfluidic techniques, and therefore the control of the number of bilayers in the polymersome structure remains an important challenge.

In this paper, we report the formation of polymersomes with double bilayers using a microfluidic technique; these

<sup>a</sup>School of Engineering and Applied Sciences and Department of Physics, Harvard University, Cambridge, Massachusetts, USA. E-mail: [weitz@seas.harvard.edu](mailto:weitz@seas.harvard.edu); Tel: +1 617-495-3275

<sup>b</sup>Department of Chemical and Biomolecular Engineering, KAIST, Daejeon, South Korea. E-mail: [kim.sh@kaist.ac.kr](mailto:kim.sh@kaist.ac.kr)

<sup>c</sup>Amore-Pacific Co. R&D Center, Yongin, South Korea

<sup>d</sup>Department of Applied Chemistry, Hanyang University, Ansan, South Korea

† Electronic supplementary information (ESI) available: Figures showing a capillary microfluidic device, microaspiration of polymersomes and overlapping of bilayers are included. In addition, movies showing generation of quadruple-emulsion drops, microaspiration of polymersomes, magnetic response of polymersomes and behavior of polymersomes subjected to osmotic shock are included. See DOI: 10.1039/c3lc41112e

provide much higher stability and lower permeability than unilamellar polymersomes. To form these new polymersomes, we develop a robust and facile two-step emulsification method to produce quadruple-emulsion drops which serve as a template for the polymersomes. Using water-in-oil-in-water-in-oil-in-water (W/O/W/O/W) quadruple-emulsion drops, we prepare polymersomes-in-polymersomes; they exhibit protrusion of the inner polymersomes through the bilayer membrane of the outer polymersomes, resulting in a budding process which leads to the formation of polymersomes with two overlapping bilayers or double bilayers. We confirm these structures are indeed double bilayers using microaspiration and selective doping of the leaflets with nanoparticles. The resultant polymersomes with double bilayers exhibit enhanced stability and reduced permeability by comparison to polymersomes with a single bilayer.

## Experimental

### Materials

A 10 wt% aqueous solution of poly(ethylene glycol) (PEG, Mw 6000, Sigma-Aldrich) is used as the innermost phase of quadruple-emulsions and a 10 wt% aqueous solution of poly(vinyl alcohol) (PVA, Mw 13 000–23 000, Sigma-Aldrich) is used as the second shell and continuous phase of quadruple-emulsions. For the amphiphile-laden oil phase used for the first and the third shells, PEG (Mw 5000)-*b*-poly(lactic acid) (PLA, Mw 10 000) diblock-copolymer (Polysciences, Inc.) is dissolved in a mixture of chloroform and hexane with a volume ratio of 38 : 62 at a concentration of 5 mg ml<sup>-1</sup>. The PLA homopolymer (Mw 15 000, Polysciences, Inc.) is added to the mixture at a concentration of 2.5 mg ml<sup>-1</sup> in some experiments. A water-soluble green dye, 8-hydroxy-1,3,6-pyrenetrisulfonic acid, trisodium salt (Spectrum Chemicals) and an oil-soluble red dye, Nile red (Aldrich) are used to observe the polymersome structure in a confocal microscope. To confirm the formation of double bilayers, we use oleic-acid-capped iron oxide nanoparticles (Fe<sub>3</sub>O<sub>4</sub>) with a diameter of 12 nm and fluorescent polystyrene microspheres with a diameter of 1 μm (FluoSphere, Invitrogen).

### Preparation of capillary microfluidic devices

The design of the device comprises three tapered cylindrical capillaries, the left, middle, and right capillaries, which are inserted in two square capillaries as shown schematically in Fig. 1a; the middle cylindrical capillary is tapered at both sides, whereas the other two cylindrical capillaries are tapered only at one side. The cylindrical capillaries are treated to render their surfaces hydrophobic or hydrophilic prior to assembly. In both junctions, the injection nozzles for the aqueous phase should be hydrophobic to prevent wetting of the aqueous phase on the nozzles, whereas the collection tubes of the resultant emulsion drops should be hydrophilic to prevent wetting of the dispersed oil phase on the collection tubes.<sup>16</sup> Therefore, the left capillary, which has a 20 μm-diameter orifice, and the right side of the middle capillary, which has a 200 μm-diameter orifice, are both treated with

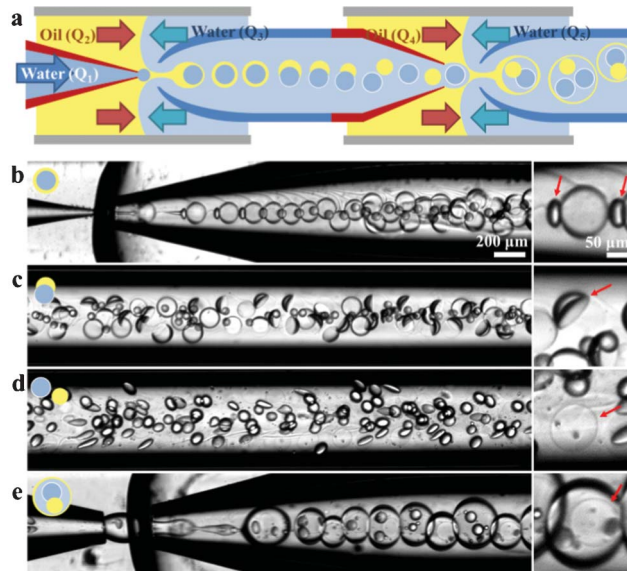


**Fig. 1** (a) Schematic illustration of the microfluidic capillary device with sequential double-emulsion drop-makers for preparation of W/O/W/O/W quadruple emulsion drops. The treatment of the surfaces of the capillaries is denoted by different colors, with red signifying a hydrophobic surface and blue signifying a hydrophilic surface, respectively. (b–e) Optical microscope images showing (b) double-emulsion generation at the first drop maker, (c) dewetting of the oil phase in the middle capillary at a distance of 2 cm from the first drop-maker, (d) separation of the oil phase in the middle capillary at a distance of 4 cm from the first drop-maker, and (e) encapsulation of the polymersomes and oil drops in the second level of double emulsion at the second drop-maker. The arrows in (b) denote satellite drops and the arrow in (c) denotes dewetting of the oil phase. The arrows in (d) and (e) denote polymersomes. The flow rates of the innermost water ( $Q_1$ ), the oil for the first shells ( $Q_2$ ), the water for the second shells ( $Q_3$ ), the oil for the third shells ( $Q_4$ ), and the water as the continuous phase ( $Q_5$ ) are kept at 0.4, 0.2, 3, 1.2, and 9 ml h<sup>-1</sup>, respectively.

hydrophobic *n*-octadecyltrimethoxysilane (OTMOS, Sigma-Aldrich) as they form the injection nozzles for the innermost aqueous phase ( $W_1$ ) and the aqueous  $W_1/O_2/W_3$  double-emulsion drops, respectively. Similarly, the left side of the middle capillary, which has a 160 μm-diameter orifice, and the right capillary, which has a 260 μm-diameter orifice, are both treated with hydrophilic 2-[methoxy(polyethyleneoxy)propyl]-trimethoxysilane (Gelest, Inc.) as they form the collection tubes of the  $W_1/O_2/W_3$  double-emulsion drops and the  $W_1/O_2/W_3/O_4/W_5$  quadruple-emulsion drops, respectively. The surface treatment is denoted as red for hydrophobic surfaces and blue for hydrophilic surfaces in Fig. 1a. For the treatment of the left and right capillaries, they are immersed in each solution of the silane coupling agent and incubated for 5 min. Following this, the solution is blown out and used. To make the left side of the middle capillary hydrophilic and the right side hydrophobic, the right side is dipped in hydrophobic silane for 3 s and vertically incubated in air for 5 min. After blowing out the residual silane, the left side is dipped in hydrophilic silane and incubated in the same manner. Once they are surface-treated, the three cylindrical capillaries are inserted in two square capillaries of the microfluidic device; the inner dimension of the square capillaries is slightly larger than the outer diameter of the cylindrical capillaries, facilitating the

coaxial alignment of the cylindrical capillaries. An image of the device is shown in Fig. S1 of the ESI.†

### Drop generation and characterization

During drop generation, flow rates are controlled by five syringe pumps (Harvard Apparatus) and the flow is observed using an inverted microscope equipped with a high speed camera (Phantom V9.0). The resultant polymersomes are collected in 50 mM aqueous solution of NaCl and are observed with a confocal laser scanning microscope (Leica, TCS SP5).

### Microaspiration experiment

Micropipette aspiration is conducted using an inverted optical microscope (Nikon TE200) equipped with a pipette micromanipulator (Narshiage MHW-3). Suction pressure of polymersomes to the micropipettes is controlled and measured with a home-built manometer and Validyne pressure transducers (Northridge, CA). Cylindrical glass capillaries of 0.9 mm in outer diameter (Friedrich and Dimmock) are tapered to be approximately 10  $\mu\text{m}$  or 30  $\mu\text{m}$  in diameter. Polymersomes are aspirated into a micropipette and the suction pressure is increased until the polymersomes rupture. During this aspiration, optical microscope images of polymersomes are recorded on video and are analyzed to obtain a stretching modulus of the polymersomes and a critical tension where they rupture (see ESI† for details).

## Results and discussion

### Generation of quadruple-emulsion drops

Multiple-emulsion drops can be formed using sequential emulsification with a series of single-drop makers, but such microfluidic devices suffer from complex assembly procedures and delicate control of flow rates to operate properly. Therefore, to overcome these shortcomings, we have developed a new design of capillary microfluidic devices for preparation of quadruple-emulsion drops; we serialize two double-emulsion makers, as shown schematically in Fig. 1a:  $W_1/O_2/W_3$  double-emulsion drops are prepared in the first junction, which then forms the innermost drop of the second level of  $W_3/O_4/W_5$  double-emulsion drops formed in the second junction. This results in  $W_1/O_2/W_3/O_4/W_5$  quadruple-emulsion drops.

Polymersomes whose membranes are composed of amphiphilic diblock-copolymers, PEG-*b*-PLA, are prepared from  $W_1/O_2/W_3/O_4/W_5$  quadruple-emulsion drops produced in these capillary devices. To accomplish this, we inject a 10 wt% aqueous solution of PEG (Mw 6000), with 100 mOsm  $\text{L}^{-1}$ , through the injection capillary of the first junction to form the innermost core drop ( $W_1$ ); any water-soluble material can be dissolved in the core drop if it does not interfere with the assembly of amphiphiles at the inner interface, and the resultant bilayer membrane of PEG-*b*-PLA does not allow diffusion of molecules with a molecular weight larger than approximately 100, thereby safely encapsulating the molecules without leakage as long as the membrane keeps its integrity.<sup>16,17,19</sup> We use a mixture of chloroform and hexane, in a

volume ratio of 38 : 62, with 5 mg  $\text{ml}^{-1}$  PEG-*b*-PLA added to form the two oil phases, the first shell ( $O_2$ ) and the third shell ( $O_4$ ). We inject this solution through the interstices of the square and the injection capillaries of both the first and the second junctions. The second shell ( $W_3$ ) and continuous phases ( $W_5$ ) are 10 wt% aqueous solution of PVA (Mw 13 000–23 000) with 100 mOsm  $\text{L}^{-1}$ ; this solution is injected through the interstices between the square and collection capillaries of both the first and the second junctions, as shown in Fig. 1a.

In the first junction, we set the flow rates of the innermost ( $Q_1$ ), the first shell ( $Q_2$ ), and the second shell ( $Q_3$ ) phases as 0.4  $\text{ml h}^{-1}$ , 0.2  $\text{ml h}^{-1}$ , and 3  $\text{ml h}^{-1}$ , respectively, to produce  $W_1/O_2/W_3$  double-emulsion drops in a dripping mode, as shown in Fig. 1b; although small satellite drops of  $O_2/W_3$  are also generated, they do not form polymersomes. The average diameter of these monodisperse double-emulsion drops is 141  $\mu\text{m}$  and its coefficient of variation (CV) is as small as 1.7%. The double-emulsion drops exhibit a dewetting of the PEG-*b*-PLA-laden oil layer on the surface of the innermost drop as they flow through the middle capillary, as shown in Fig. 1c; this is caused by fast diffusion of chloroform from the oil shell to the continuous water phase. The increase of the hexane concentration which is a poor solvent for PEG-*b*-PLA decreases the interfacial tension due to promoted adsorption of the diblock-copolymers at the interface. In addition, reduction of solvent quality leads to an attraction between the PLA blocks; this long-range force causes that the PLA blocks of diblock-copolymers at the two interfaces are brought into contact to reduce the energy. Therefore, unbalanced forces at the dewetting front lead to a negative spreading parameter of the oil phase, thereby expelling the oil phase with low solvent quality from the innermost drop.<sup>20</sup> The dewetted oil drops containing excess of the PEG-*b*-PLA spontaneously separate from the innermost drops, leaving unilamellar polymersomes downstream, in the middle capillary, as shown in Fig. 1d. Finally, the polymersomes and the oil drops are encapsulated in the second level of the  $W_3/O_4/W_5$  double-emulsion drops at the second junction, which has flow rates of the third oil shell ( $Q_4$ ) and the continuous phases ( $Q_5$ ) of 1.2  $\text{ml h}^{-1}$  and 9  $\text{ml h}^{-1}$ , respectively, as shown in Fig. 1e. The  $W_3/O_4/W_5$  double-emulsion drops are produced by a breakup of a widening coaxial jetting; injected inner polymersomes perturb the jet and induce its breakup.<sup>17</sup> Although such inner-polymersome-triggered breakup makes polydisperse double-emulsion drops due to inconsistent injection frequency of the inner polymersomes, it enables that the majority of the resultant double-emulsion drops encapsulate only one inner polymersome per drop, as shown in Fig. 1e; approximately 70% of drops have one inner polymersome and 20% of them have no polymersome. This is very important for production of the polymersomes with double bilayers through a budding process; when we produce monodisperse outer double-emulsion drops containing an uncontrolled number of inner polymersomes, the inner polymersomes frequently escape without protrusion and budding due to the insufficient area of the outer bilayer. The average diameter of these polydisperse double-emulsion drops is 282  $\mu\text{m}$  and its CV is 13.4%. Each of these steps is shown in supplementary movie 1 of the ESI;† the last part of

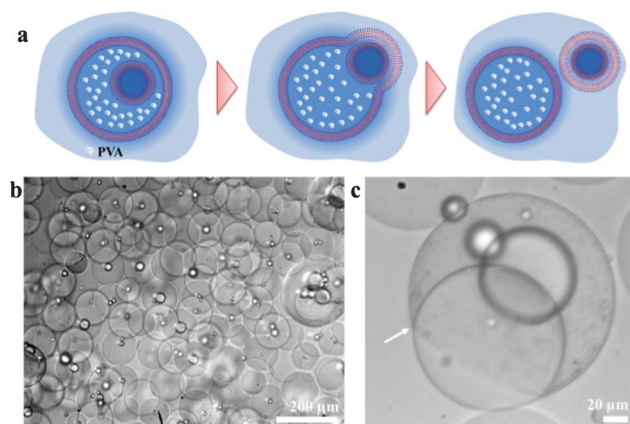


**Fig. 2** (a) Schematic illustration of the depletion-induced overlapping of two bilayers in polymersomes-in-polymersomes and the budding of the inner polymersome through the outer polymersome. (b, c) Optical microscope images of polymersomes templated from quadruple-emulsion drops. The arrow in (c) denotes protrusion of the inner polymersome through the outer polymersome by overlapping two bilayers.

the movie shows inner-polymersome-triggered breakup and encapsulation of one inner polymersome per drop.

### Formation of double bilayers

The outer  $W_3/O_4/W_5$  double-emulsion drops exhibit dewetting and separation of oil drops in a fashion similar to that of the inner  $W_1/O_2/W_3$  double-emulsion drops; this results in the formation of a polymersome-in-polymersome structure. However, we observe protrusion of the inner polymersomes through the bilayer of the outer polymersomes; we attribute this to the depletion-induced attraction between the two bilayers of the inner and outer polymersomes, where PVA molecules in the second shell ( $W_3$ ) play the role of depletants, as shown schematically in Fig. 2a. In addition, there is a small amount of residual oil in the bilayer which makes the membrane very flexible; this extremely low stretching modulus of the PEG-*b*-PLA bilayer immediately after its formation facilitates deformation of the bilayer. Although we intentionally rupture the polymersomes with mechanical strain to estimate the amount of residual oil, the ruptured polymersomes do not form spherical drops but behave like a highly flexible solid membrane; this indicates that the amount of residual oil is very small. We use microaspiration to verify the existence of residual oil in polymersome membranes and measure the stretching modulus, as was demonstrated by Kamat *et al.*<sup>21,22</sup> the polymersome with residual oil, stored for 12 h in a closed chamber to minimize evaporation of the oil, has a stretching modulus that is measured to be as small as  $8.7 \pm 1.9 \text{ mN m}^{-1}$ . By contrast, the polymersome, incubated for a week in an open chamber, has a stretching modulus that is measured to be  $136 \pm 32.5 \text{ mN m}^{-1}$ , as shown in Fig. S2 of the ESI,<sup>†</sup> which is comparable with the modulus of a unilamellar membrane of polymersomes.<sup>13</sup> Further incubation makes insignificant changes in the modulus, which means that the residual oil is completely removed.<sup>22</sup> We also observe overlapping of two bilayers between single polymersomes

dispersed in an aqueous solution of 6 wt% PVA and 25 mM NaCl as shown in Fig. S3, ESI.<sup>†</sup> These single polymersomes adhere to each other, forming a double bilayer in the portion of the membrane that separates them; this is similar to the double bilayer in the polymersomes-in-polymersomes.<sup>21</sup> We think that a small amount of water might be trapped between two bilayers during the adhesion. Finally, the protruded inner polymersomes separate from the outer polymersomes, forming double bilayers. The polymersomes with double bilayers prepared by budding of the inner polymersome from the outer polymersomes are shown in Fig. 2b and Fig. S4, ESI;<sup>†</sup> approximately 80% of the inner polymersomes exhibit complete separation. Some of the polymersomes are fixed during protrusion; the boundary between double and single bilayers is denoted by an arrow as shown in Fig. 2c. When the diameter of the inner polymersome is close to that of the outer polymersome, the polymersome-in-polymersome structures remain in the form of concentric shells without protrusion, as denoted with circles in Fig. S5, ESI;<sup>†</sup> this is attributed to the reduction of the depletion attraction due to the similar curvatures of each of the two bilayers. The resultant polymersomes are a mixture of double-bilayer polymersomes and single-bilayer polymersomes as shown in Fig. S4, ESI.<sup>†</sup>

### Confirmation of double bilayers

Formation of double bilayers is confirmed by aspirating the polymersomes with a microcapillary as shown schematically in Fig. S6a of the ESI;<sup>†</sup> direct observation of the budding process is difficult because it quickly occurs within collection tubing. When the polymersomes are reinforced by adding PLA homopolymers into the hydrophobic part of the single bilayer,<sup>17</sup> they exhibit a very high modulus which is difficult to measure by aspiration due to insignificant deformation even up to a critical tension of  $74 \text{ mN m}^{-1}$ , where the membrane ruptures. The polymersomes composed of double bilayers with PLA homopolymer in the hydrophobic regions of both bilayers also show negligible deformation, as shown in Fig. S6b, ESI;<sup>†</sup> however, the critical tension is almost doubled to  $135 \text{ mN m}^{-1}$ . In addition, the double bilayers exhibit sudden deformation of the membrane right before rupture; optical contrast of the membrane also suddenly becomes much weaker here, as shown in Fig. S6c, ESI.<sup>†</sup> A similar effect is not observed for polymersomes with a single bilayer. We attribute the sudden deformation and the loss of optical contrast to the selective rupture of the outer bilayer; we think that a small amount of water trapped between the two bilayers facilitates this selective rupture. As soon as the outer bilayer ruptures, the inner bilayer is quickly deformed due to the very high tension, and, because the pressure is above its critical pressure, it ruptures. This microaspiration of the polymersome with double bilayers is shown in supplementary movie 2 of the ESI.<sup>†</sup>

Overlapping of the bilayers is also confirmed by selective doping of nanoparticles into the outer bilayer. Hydrophobic magnetic nanoparticles of 12 nm in diameter, capped with oleic acid, are dispersed only in the third oil shell phase ( $O_4$ ) of the quadruple-emulsion drops; they are trapped in the hydrophobic part of the outer bilayer during the dewetting of the oil phase.<sup>23</sup> When the inner polymersomes make double

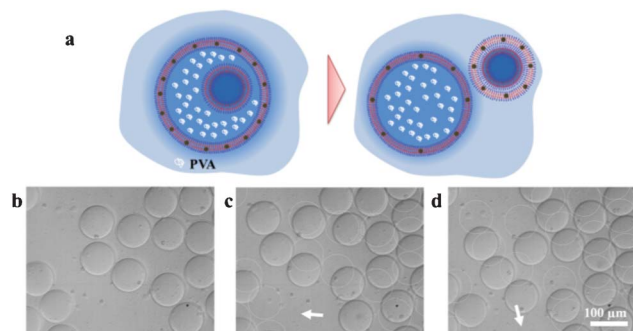


**Fig. 3** (a) Schematic illustration of the budding of the inner polymersomes where the bilayer of the outer polymersome is doped with magnetic nanoparticles. (b–d) Optical microscope images of the polymersomes produced by budding from outer polymersomes with a magnetic particle-doped bilayer. The polymersomes migrate upon application of a magnetic field, where arrows denote the direction of the magnetic field. To guide the eye, the positions of polymersomes before application of the magnetic field are denoted with circles in (c) and (d).

bilayers during protrusion and budding, the resultant polymersomes will therefore be magneto-responsive, as shown schematically in Fig. 3a. When we apply a magnetic field to the polymersomes produced from quadruple-emulsion drops, they move toward the magnet, as shown in Fig. 3b–d and supplementary movie 3 of the ESI;† in the same manner, the leaflets of inner polymersomes can be selectively doped with magnetic nanoparticles; this potentially enables the separation of the polymersomes with double bilayers from the mixture of polymersomes using an external magnetic field. In addition, when the second water shell phase ( $W_3$ ) contains fluorescent polystyrene particles of 1  $\mu\text{m}$  in diameter, we also observe trapping of a few particles between the overlapping bilayers, as shown in Fig. S7, ESI.† This is evidence of the formation of double bilayers.

### Properties of double bilayers

The polymersomes composed of double bilayers have higher stability and lower permeability than those composed of a single bilayer. We confirmed this by applying an osmotic shock to the polymersomes. When polymersomes with an aqueous core of PEG, with 0.1  $\text{Osm L}^{-1}$ , are subjected to the osmotic shock imposed by an aqueous solution of NaCl at 2  $\text{Osm L}^{-1}$ , we observe that they initially deflate due to outward flow of water through the membrane; however they subsequently begin to re-inflate to a spherical shape, as shown in Fig. 4. We attribute this re-inflation to the fast diffusion of sodium and chloride ions into the interior of the polymersomes after rupture of the membranes.<sup>17</sup> Under the high osmotic shock, the membrane is torn and the ions in the continuous phase can quickly diffuse into the interior of the polymersomes through the tear; by contrast, the PEG molecules originally encapsulated within the core remain, due to their relatively low mobility. This results in a higher net osmolarity in the interior of the polymersomes than in the exterior. Due to their ability to self-heal,<sup>24</sup> the deflated polymersomes are re-inflated by the inward flow of water from the continuous phase. This process is illustrated

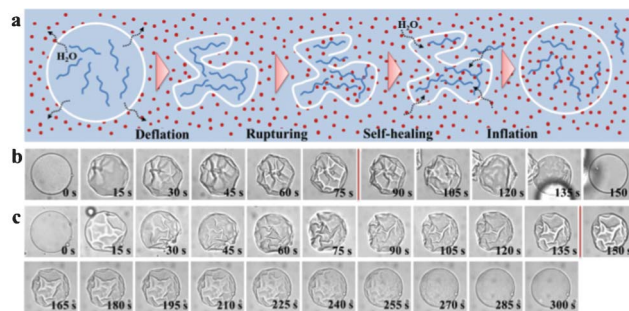


**Fig. 4** (a) Schematic illustration of the response of a polymersome subjected to an osmotic shock. Polymersomes deflate as soon as the shock is applied, but subsequently re-inflate to a spherical shape. (b, c) Series of optical microscope images showing initial deflation and subsequent re-inflation of a polymersome templated (b) by double-emulsion drops and (c) by quadruple-emulsion drops in an aqueous solution of NaCl at 2  $\text{Osm L}^{-1}$ . The images are taken at the denoted time in each image with an interval of 15 s and the red lines denote the rough boundary between the deflation and the re-inflation.

schematically in Fig. 4a. Although polymersomes with both single and double bilayers exhibit similar behavior, the rate of deflation and re-inflation is different. The polymersomes with double bilayers exhibit slower deflation and re-inflation than the polymersomes with a single bilayer by a factor of approximately 2; a polymersome with a single bilayer deflates in 75 s and re-inflates in a further 75 s, as shown in Fig. 4b, whereas a polymersome with a double bilayer deflates in 135 s and re-inflates in a further 165 s, as shown in Fig. 4c and supplementary movie 4 of the ESI.† We attribute this to the reduced permeability of the membrane of double bilayers.

## Conclusions

In this work, we report a pragmatic microfluidic approach to create quadruple-emulsion drops which serve as templates to produce polymersomes with double bilayers. When two bilayer membranes are attracted by depletion in polymersomes-in-polymersomes structures, the inner polymersomes protrude and bud, forming double bilayers. The resultant polymersomes exhibit enhanced stability and reduced permeability. Therefore, polymersomes with double bilayers are potentially useful as highly stable and biocompatible microcarriers for robust encapsulation and long-term storage of bioactives such as drugs, cosmetics, and nutrients; this is otherwise difficult to achieve with liposomes or even with unilamellar polymersomes. In addition, this microfluidic approach could be potentially used to produce polymersomes with triple or more bilayers by simply increasing the number of double-emulsion generators and a variety of amphiphilic diblock-copolymers including PEG–PLA, PAA–PBA<sup>15</sup> and PEG–PS<sup>25</sup> could be potentially used to make such multi-bilayers. Moreover, the polymersome membranes can be doped by magnetic nanoparticles, enabling their magnetic manipulation; in the same fashion, metal nanoparticles could be also incorporated,

which would provide a light-triggered rupture of the membrane using the photothermal effect.<sup>26,27</sup>

## Acknowledgements

This work was supported by Amore-Pacific, the NSF (DMR-1006546) and the Harvard MRSEC (DMR-0820484). We appreciate Prof. Jaeyun Kim in SKKU for providing iron oxide nanoparticles.

## Notes and references

- 1 S. Okushima, T. Nisisako, T. Torii and T. Higuchi, *Langmuir*, 2004, **20**, 9905–9908.
- 2 A. S. Utada, E. Lorenceau, D. R. Link, P. D. Kaplan, H. A. Stone and D. A. Weitz, *Science*, 2005, **308**, 537–541.
- 3 A. R. Abate and D. A. Weitz, *Small*, 2009, **5**, 2030–2032.
- 4 S. H. Kim and D. A. Weitz, *Angew. Chem., Int. Ed.*, 2011, **50**, 8731–8734.
- 5 L. Y. Chu, A. S. Utada, R. K. Shah, J. W. Kim and D. A. Weitz, *Angew. Chem., Int. Ed.*, 2007, **46**, 8970–8974.
- 6 S. W. Choi, Y. Zhang and Y. N. Xia, *Adv. Funct. Mater.*, 2009, **19**, 2943–2949.
- 7 Y. Hennequin, N. Pannacci, C. P. de Torres, G. Tetradis-Meris, S. Chapuliot, E. Bouchaud and P. Tabeling, *Langmuir*, 2009, **25**, 7857–7861.
- 8 J. W. Kim, A. S. Utada, A. Fernandez-Nieves, Z. B. Hu and D. A. Weitz, *Angew. Chem., Int. Ed.*, 2007, **46**, 1819–1822.
- 9 S. H. Kim, S. J. Jeon and S. M. Yang, *J. Am. Chem. Soc.*, 2008, **130**, 6040–6046.
- 10 S. H. Kim, J. W. Kim, J. C. Cho and D. A. Weitz, *Lab Chip*, 2011, **11**, 3162–3166.
- 11 D. Lee and D. A. Weitz, *Adv. Mater.*, 2008, **20**, 3498–3503.
- 12 S. H. Kim, H. Hwang, C. H. Lim, J. W. Shim and S. M. Yang, *Adv. Funct. Mater.*, 2011, **21**, 1608–1615.
- 13 B. M. Discher, Y. Y. Won, D. S. Ege, J. C. M. Lee, F. S. Bates, D. E. Discher and D. A. Hammer, *Science*, 1999, **284**, 1143–1146.
- 14 D. E. Discher and F. Ahmed, *Annu. Rev. Biomed. Eng.*, 2006, **8**, 323–341.
- 15 E. Lorenceau, A. S. Utada, D. R. Link, G. Cristobal, M. Joanicot and D. A. Weitz, *Langmuir*, 2005, **21**, 9183–9186.
- 16 H. C. Shum, J. W. Kim and D. A. Weitz, *J. Am. Chem. Soc.*, 2008, **130**, 9543–9549.
- 17 S. H. Kim, H. C. Shum, J. W. Kim, J. C. Cho and D. A. Weitz, *J. Am. Chem. Soc.*, 2011, **133**, 15165–15171.
- 18 A. Perro, C. Nicolet, J. Angy, S. Lecommandoux, J. F. Le Meins and A. Colin, *Langmuir*, 2011, **27**, 9034–9042.
- 19 H. C. Shum, Y. J. Zhao, S. H. Kim and D. A. Weitz, *Angew. Chem., Int. Ed.*, 2011, **50**, 1648–1651.
- 20 H. C. Shum, E. Santanach-Carreras, J. W. Kim, A. Ehrlicher, J. Bibette and D. A. Weitz, *J. Am. Chem. Soc.*, 2011, **133**, 4420–4426.
- 21 J. Nam and M. M. Santore, *Langmuir*, 2007, **23**, 7216–7224.
- 22 N. P. Kamat, M. H. Lee, D. Lee and D. A. Hammer, *Soft Matter*, 2011, **7**, 9863–9866.
- 23 W. H. Binder, R. Sachsenhofer, D. Farnik and D. Blaas, *Phys. Chem. Chem. Phys.*, 2007, **9**, 6435–6441.
- 24 O. Sandre, L. Moreaux and F. Brochard-Wyart, *Proc. Natl. Acad. Sci. U. S. A.*, 1999, **96**, 10591–10596.
- 25 R. C. Hayward, A. S. Utada, N. Dan and D. A. Weitz, *Langmuir*, 2006, **22**, 4457–4461.
- 26 A. P. Esser-Kahn, S. A. Odom, N. R. Sottos, S. R. White and J. S. Moore, *Macromolecules*, 2011, **44**, 5539–5553.
- 27 E. Amstad, S.-H. Kim and D. A. Weitz, *Angew. Chem., Int. Ed.*, 2012, **51**, 12499–12503.